Resilience of parity-violation-induced chiral selectivity to nonequilibrium temperature fluctuations in open systems

David Hochberg ◉,[1,*] Thomas Buhse ◉,[2] Jean-Claude Micheau ◉,[3] and Josep M. Ribó ◉[4,†]

[1]*Department of Molecular Evolution, Centro de Astrobiología (CSIC-INTA), Carretera Ajalvir Kilómetro 4,*
28850 Torrejón de Ardoz, Madrid, Spain

[2]*Centro de Investigaciones Químicas, IICBA, Universidad Autónoma del Estado de Morelos, 62209 Cuernavaca, Morelos, Mexico*

[3]*Laboratoire des IMRCP, UMR au Centre National de la Recherche Scientifique No. 5623,*
Université Paul Sabatier, F-31062 Toulouse, France

[4]*Department of Inorganic and Organic Chemistry, Organic Chemistry Section, Institute of Cosmos Science, Universitat de Barcelona*
(IEEC-ICC), C. Martí i Franqués 1, E-08028 Barcelona, Catalonia, Spain

We consider the sensitivity of chemical reactions, able to undergo spontaneous mirror symmetry breaking, to chiral bias in the presence of nonequilibrium temperature fluctuations and derive a selectivity criterion. For this, we estimate the magnitude of fluctuations δk in chemical reaction rate constants k arising from the nonequilibrium temperature fluctuations δT about a mean value T. To leading order, the relative rate constant fluctuations $\delta k_i/k_i$ for each reaction i are given by the product of the activation enthalpy $\Delta H_i^{\ddagger}/RT$ for the ith reaction multiplied by the relative rms temperature fluctuations $\delta T_{rms}/T$. The latter are determined by the system's specific heat at constant volume: C_V. We test this criterion with simulations carried out for an open-flow fully reversible Frank model, and for a range of parity-violating energy differences (PVED) within the theoretically estimated upper and lower bounds. Depending on the relative magnitudes of the deterministic PVED bias and the temperature fluctuations, the PVED bias can either (i) select the final stable chiral outcome deterministically or (ii) select one of two possible stable chiral outcomes with an asymmetric statistical weighting. For larger temperature fluctuations, the PVED bias loses its selectivity, and the final stable chiral outcomes are stochastic and equally probable. This paper points towards the possible design of small volume chemical flow reactors capable of detecting the elusive PVED bias in bulk systems, provided other sources of fluctuations can be sufficiently controlled and attenuated.

I. INTRODUCTION

The homochirality of biological molecules is a basic signature of life and is based on a remarkable spatial asymmetry, namely, on one of the two enantiomers of chiral sugars and chiral amino acids. Enantiomers are molecules with identical chemical structure but the mirror images of which are not superimposable. This biological homochirality was discovered by Pasteur in 1857, but its origin (or perhaps origins) still remains elusive after more than 170 years and has spurred an intense research activity nurtured from the investigations made in the fields of chemistry and physics [1]. According to Crick, "The first great unifying principle of biochemistry is that the key molecules have the same hand in all organisms" [2]. The primordial nature of the *origin* of mirror symmetry

breaking at the molecular level, which through subsequent amplification and chirality transfer through chemical transformations leads to the dominance of one hand over the other, can be either chance or deterministic. The former includes the inherent statistical compositional fluctuations about the ideal racemic configuration (perfect mirror symmetry), thermal fluctuations, and also external noise. The latter refers to a physical chiral influence which creates an enantiomeric imbalance, or bias, in an otherwise achiral composition [1]. Of all possible chiral influences, only the parity-violating weak interaction is *universal*, in that it exists for matter everywhere in space, and for all times subsequent to the symmetry breaking transition from a putative grand unified model down to the standard model of particle physics [3].

Parity violation in the weak interaction was first suggested to be the origin of this biological chirality already in the 1960s, thus determining the preference of the enantiomers selected by nature, that is, the D sugars and the L amino acids [4,5]. The associated parity-violating energy difference (PVED) has been studied and calculated in recent years, and the estimated value of the parity-violating energy shift (E_{PV}) between enantiomers (pairs of single molecules of opposite handedness), based on electroweak quantum chemistry, is several orders of magnitude smaller than current experimental resolution [6]. This is the situation in so far as individual

*hochbergd@cab.inta-csic.es
†jmribo@ub.edu

chiral molecules are concerned. However, this does not rule out the possibility of being able to detect a physical chiral bias induced by PVED, and on the level of bulk macroscopic chemical systems. Chemical reaction systems based on enantioselective autocatalysis are able to undergo mirror symmetry breaking and lead to a stochastic (random) distribution of chiral signs (i.e., left or right handed outcomes) between experiments, due to the stochastic distribution of signs in the inherent fluctuations. In contrast, a physical chiral polarization (such as PVED, polarized light, or hydrodynamic vortices in three dimensions) can select deterministically the final stable chiral sign, provided the chiral bias can overcome the opposing random fluctuations. In either situation, the mirror symmetry breaking, whether it be random or deterministic, is a joint *collective* property of the bulk macroscopic system.

The sensitivity of nonequilibrium chemical systems to symmetry breaking influences, in the presence of chiral fluctuations in the chemical composition and at the critical point of the bifurcation, was investigated in detail by Kondepudi and Nelson decades ago [7,8]. Those pioneering studies were concerned with fluctuations in the *numbers* of molecules, while keeping both the temperature T and the volume V constant. Nevertheless, far from equilibrium open systems are subject to fluctuations in the temperature, the volume, and the number of chemical species [9,10]. In particular, temperature fluctuations are always present to some degree in all systems, and these lead directly to fluctuations in the reaction rate constants. It is therefore important to explore their impact on chemical systems able to undergo symmetry breaking transitions, and to be able to characterize the sensitivity of such systems to deterministic chiral influences and bias. In contrast to those previous studies, we do not assume the chemical system to be located exactly at its critical point, nor that it necessarily passes through its critical point, say under the continuous variation of some external parameter. We do consider a system which is located initially in a nonequilibrium racemic configuration, and at some arbitrary finite distance from the putative critical point without implying a purposeful or deliberate adjustment or variation of external parameters. Such an initial condition is determined by the model parameters, the reaction rate constants, the flow rates and the initial chemical compositions, etc. That is, we envisage that a chemical system with enantiomers may well start off in a state of ideal racemic composition, which could be a stable nonequilibrium stationary state (NESS, i.e., racemate) or an unstable one, or even a nonstationary state, but without necessarily having had to transit through any critical point, in analogy to the analysis of spontaneous mirror symmetry breaking in the absence of chiral bias, where the system is initially located on the unstable racemic (or, thermodynamic) branch. We thus aim to consider the chiral selection problem in this more general setting, and under the influence of a PVED competing with the omnipresent random temperature fluctuations. The latter involves taking into account fluctuating reaction rate constants. The corresponding noise is therefore multiplicative.

Bifurcation theory applied to the chiral symmetry breaking problem in molecular systems has revealed important distinctions regarding the stability in the presence or absence of physical chiral interactions [7,8]. In the absence of such interactions, and provided the system is out of equilibrium,

the racemic (thermodynamic) branch can become unstable, due to the increase in the entropy production in being far from equilibrium. The slightest fluctuation thus perturbs the system so as to evolve to one of two otherwise equally probable final stable scalemic states. Which final state the system ends up in is determined solely by the chiral sign of initial random fluctuation. While each such individual outcome is scalemic, the average over the ensemble of these stochastically distributed scalemic outcomes yields a net racemic outcome. By marked contrast, in the presence of a physical chiral interaction, the racemic configuration is no longer an unstable stationary state, but instead now lies within the basin of attraction of only one of the two final stable scalemic branches. This is because in the presence of a chiral bias, the thermodynamic branch is no longer racemic, but is now scalemic and also stable (see Appendix D). Thus, if there were no fluctuations, the system initiated on a racemic configuration would therefore always evolve *deterministically* to one and the same final stable scalemic state. It is in this sense that the deterministic chiral interaction, or bias, selects the outcome. However, in the presence of temperature fluctuations, the chiral bias can be a good selector of the final scalemic outcome only if it can overcome the influence of the nonequilibrium fluctuations. In fact, the chiral bias must be able to overcome the fluctuations that might otherwise knock the initially racemic configuration so as to cause the system to evolve in the *opposite* direction towards the *other* stable scalemic branch of the imperfect bifurcation (see Appendix D).

We analyze in detail the competition between the nonequilibrium temperature fluctuations and the deterministic chiral bias imposed by the PVED in enantiomers. We explore numerically the conditions for the PVED to act as a selector of the final stable scalemic state in the presence of temperature fluctuations around an initial nonequilibrium racemic configuration, and for a range of currently accepted PVED values. That is, in the presence of temperature fluctuations, we ask what is the *minimum* value of the PVED energy difference required for selecting one of the two possible stable chiral outcomes? To answer this, we consider a fully reversible Frank reaction scheme kept out of equilibrium by open flow in a continuous stirred tank reactor. Moreover, the Frank paradigm itself (i.e., enantioselective autocatalysis and mutual inhibition) is known to lie at the heart of the Soai reaction [11], and hence lessons learned from the competition between fluctuations and chiral bias in a simple enantioselective autocatalytic model with mutual inhibition provide proof of concept for analyzing and assessing the chiral selectivity problem in more intricate experimental and theoretical Frank-paradigm models that are able to capture the essential mechanistic and kinetic aspects of the Soai reaction mechanism [12–16].

For a given value of the PVED, its ability to effect symmetry breaking consistently in one direction (deterministic outcome) will be compromised at some critical value of the root mean square temperature fluctuations. Beyond this value, the reaction outcome becomes stochastic, just as expected in the absence of a chiral bias. The aim of this paper is to quantify these noise threshold values, induced in the reaction rate constants, and for the case of the reaction model employed.

To this end, in Sec. II A we consider how the rate constant fluctuations are driven by those in the temperature.

Thermodynamic constraints, in Sec. III, play a crucial role in symmetry breaking, and are broken in the presence of temperature fluctuations, although the level of breaking is minuscule, of second order in the relative temperature fluctuation. We next define the open-flow reversible Frank model and its stochastic version in Sec. IV. This is followed in Sec. V by a derivation of the PVED selectivity criterion. For a given reaction, the bias g induced by the PVED in the rate constant is compared to the temperature induced fluctuation ξ in that same rate constant. Then selectivity, deterministic outcome, is expected when $g > \xi$. This criterion is tested out in simulations of the stochastic Frank model in Sec. VI, where the salient results obtained regarding selectivity are discussed when $g > \xi$, $g \approx \xi$, and $g < \xi$, and also the residual persistent bias. Simple order-of-magnitude estimates for the minimum size of a possible small laboratory scale PVED "detector" are given in Sec. VII. Discussion is provided in Sec. VIII.

II. RATE CONSTANT DEPENDENCE ON TEMPERATURE FLUCTUATIONS

A. The Eyring-Polanyi equation

From transition state theory, the rate constant of a reaction is written as (see, e.g., Chap 9 in [10] and Chap 12 in [17])

$$k(T) = \frac{k_B T}{h} e^{-\frac{\Delta G^{\ddagger}}{RT}} \left(M^{(1-m)} s^{-1} \right) \qquad (1)$$

where $\Delta G^{\ddagger} = G^0(\text{activated complex}) - G^0(\text{reactants}) > 0$ for forward reactions, and $\Delta G^{\ddagger} = G^0(\text{activated complex}) - G^0(\text{products}) > 0$, for reverse reactions, that is, the free energies of activation (see, e.g., typical reaction coordinate diagrams [17]). R is the gas constant and T is the *mean* temperature. Since at temperature T the molecules have energies given by a Boltzmann distribution, one can expect the number of collisions with energy greater than $\Delta G^{\ddagger}$ to be proportional to $e^{-\frac{\Delta G^{\ddagger}}{RT}}$. We write the units, where M is the molarity and m is the molecularity of the reaction, e.g., m = 1, 2 for unimolecular, for bimolecular, etc. [17]. The preexponential factor can be readily calculated; thus, for example, at room temperature,

$$\frac{k_B T}{h} = (1.3881 \times 10^{-23} \text{ J K}^{-1})(300 \text{ K})/(6.626 \times 10^{-34} \text{ J s})$$
$$= 6.25 \times 10^{12} \text{ s}^{-1}. \qquad (2)$$

Consider temperature *fluctuations* $T \pm \delta T$, such that $|\frac{\delta T}{T}| \ll 1$. Then, expanding $k(T)$ for small relative temperature fluctuations $|\frac{\delta T}{T}| \ll 1$ we find (see Appendix A) to leading order

$$k(T \pm \delta T) = k(T)\left\{ 1 \pm \frac{\Delta H^{\ddagger}}{RT} \frac{\delta T}{T} + O\left[\left(\frac{\delta T}{T}\right)^2 \right] \right\}, \quad (3)$$

where $\Delta G^{\ddagger} = \Delta H^{\ddagger} - T\Delta S^{\ddagger}$ relates the activation energy to the activation enthalpy $\Delta H^{\ddagger}$ and activation entropy $\Delta S^{\ddagger}$.

Defining $\delta k(T) = k(T \pm \delta T) - k(T)$ shows that the relative fluctuations in the rate constants are given by

$$\frac{\delta k(T)}{k(T)} \simeq \pm \frac{\Delta H^{\ddagger}}{RT} \frac{\delta T}{T}. \qquad (4)$$

The relative fluctuations in k are directly proportional to the relative fluctuations in T, and the proportionality factor is the transition state enthalpy of activation for the specific chemical reaction in question, divided by RT.

To estimate the *characteristic amplitude* of the temperature fluctuations, we use the following result from statistical physics [18] for the mean square temperature fluctuation (see Appendix B):

$$\langle (\delta T)^2 \rangle = \frac{k_B T^2}{C_V} \qquad (5)$$

$$\Rightarrow \delta T_{\text{rms}} \equiv \sqrt{\langle (\delta T)^2 \rangle} = \sqrt{\frac{k_B}{C_V}} \, T, \qquad (6)$$

$$\frac{\delta T_{\text{rms}}}{T} = \sqrt{\frac{k_B}{C_V}}, \qquad (7)$$

where C_V is the specific heat at constant volume and δT_{rms} the root mean square. The time-dependent temperature fluctuations, within one standard deviation of the mean value, satisfy $|\delta T(t)| \lesssim \delta T_{\text{rms}}$.

We substitute this back into Eq. (3) and find that the corresponding fluctuating rate constant is given by

$$\boxed{k[T \pm \delta T(t)] = k(T)\left(1 + \frac{\Delta H^{\ddagger}}{RT} \sqrt{\frac{k_B}{C_V}} \, \eta(t) \right)}, \qquad (8)$$

where $\eta(t)$ is a uniformly distributed random variable in the range $[-1, 1]$, a white noise which accounts for the $\pm$ sign in Eq. (3) implicitly.

A few remarks concerning Eq. (8) are in order. The temperature fluctuations are Gaussian distributed according to Eq. (B7); the width of this probability distribution is characterized by its standard deviation; the latter is also the mean of the square of the temperature fluctuations [see Eq. (B8)]. The approximation in arriving at Eq. (8) consists in using this standard deviation to estimate the characteristic scale of the time-dependent temperature fluctuations, and we consider the random temperature fluctuations in the range $-\delta T_{\text{rms}} < \delta T(t) < \delta T_{\text{rms}}$. We implement the latter inequality by writing $\delta T(t) = \delta T_{\text{rms}} \eta(t)$, for a uniformly distributed random variable η in the range $[-1, 1]$. Thus, the overall approximation consists in considering temperature fluctuations within one standard deviation of the mean temperature, and approximating the Gaussian by a uniform distribution (by a step function) in this range.

The amplitude ξ of the rate constant fluctuations is given by

$$\xi = \frac{\Delta H^{\ddagger}}{RT} \sqrt{\frac{k_B}{C_V}} > 0, \qquad (9)$$

and substituting into Eq. (8) leads to

$$k_i[T \pm \delta T(t)] = k_i(T)[1 + \xi_i \, \eta_i(t)], \qquad (10)$$

where we emphasize that both amplitude ξ_i and noise η_i depend on the ith reaction.

Appendix B reviews the calculation of the nonequilibrium temperature fluctuations according to a suitable normal distribution [10].

TABLE I. Estimates of the free energies of activation at $T = 300$ K.

k (M$^{(1-\mathrm{m})}$ s^{-1})	$\frac{\Delta G^{\ddagger}}{RT}$	$\Delta G^{\ddagger}$ (kJ/mol)
$k_d = 10^{-4}$	38.67	96.68
$k_{-d} = 10^{-9}$	50.19	125.47
$k_a = 10^{2}$	24.86	62.15
$k_{-a} = 10^{-3}$	36.37	90.93
$k_1 = 10^{2}$	24.86	62.15
$k_{-1} = 10^{-4}$	38.67	96.68

B. Some numerical estimates

Temperature fluctuations lead to corresponding fluctuations in the reaction rate constants, and their influence can be modeled by multiplicative noise. This was assumed to be the case some time ago [19], except here we give this a fundamental physicochemical basis and, even more importantly, we can actually calculate the magnitude of these fluctuations in chemical systems in a rigorous fashion (see Appendix B).

Given a rate constant k, we can calculate the corresponding free energies of activation using the Eyring-Polanyi formula Eq. (1) since

$$-\ln\left(\frac{k}{k_B T/h}\right) = \frac{\Delta G^{\ddagger}}{RT}. \tag{11}$$

The values chosen for the forward and reverse rates of direct production k_d and k_{-d}, the forward and reverse rates of enantioselective autocatalysis k_a and k_{-a}, and the rates of heterodimerization and heterodimer dissociation k_1 and k_{-1} that were used in the simulations of the Frank model (see Sec. IV) are collected in Table I, with the corresponding free energies of activation differences at room temperature. The major point worth emphasizing here is that, although the individual rate constants themselves can range over many orders of magnitude, the associated normalized activation energies $\frac{\Delta G^{\ddagger}}{RT}$ can nevertheless all be of the *same* order of magnitude (see Table I) and therefore, by virtue of Eq. (9), so likewise for the corresponding noise amplitudes ξ, in the approximation that $\Delta G^{\ddagger} \approx \Delta H^{\ddagger}$, since the thermodynamic factor $\sqrt{\frac{k_B}{C_V}}$ is common to all of them.

III. TEMPERATURE FLUCTUATIONS AND THERMODYNAMIC CONSTRAINTS

From Eq. (10) we express each individual rate constant as $k_i = \bar{k}_i[1 + \xi_i \eta_i(t)]$ where $\bar{k}_i$ is the average value, ξ_i is the noise amplitude, $\langle \eta_i(t) \rangle = 0$, and $\langle \eta_i(t) \eta_j(t) \rangle = \delta_{ij}$, the latter indicating the noise functions for distinct chemical transformations are independent. Then since $\langle k_i \rangle = \bar{k}_i$, the ratio of the average values satisfies

$$\frac{\langle k_i \rangle}{\langle k_{-i} \rangle} = \frac{\bar{k}_i}{\bar{k}_{-i}} = K_i^{\mathrm{eq}}, \tag{12}$$

where K_i^{eq} is the deterministic equilibrium constant of the ith reversible reaction. But this may differ from the average of the

fluctuating equilibrium constant, so let us consider

$$
\begin{aligned}
\langle K_i^{\mathrm{eq}}(t) \rangle &\equiv \left\langle \frac{k_i}{k_{-i}} \right\rangle = \left\langle \frac{\bar{k}_i(1 + \xi_i\,\eta_i(t))}{\bar{k}_{-i}(1 + \xi_{-i}\,\eta_{-i}(t))} \right\rangle \\
&= \frac{\bar{k}_i}{\bar{k}_{-i}} \left\langle \frac{(1 + \xi_i\,\eta_i(t))}{(1 + \xi_{-i}\,\eta_{-i}(t))} \right\rangle \\
&= \frac{\bar{k}_i}{\bar{k}_{-i}} \left\langle (1 + \xi_i\,\eta_i(t))(1 + \xi_{-i}\,\eta_{-i}(t))^{-1} \right\rangle \\
&= \frac{\bar{k}_i}{\bar{k}_{-i}} \left\langle (1 + \xi_i\,\eta_i(t))\left(1 - \xi_{-i}\,\eta_{-i}(t)\right. \right. \\
&\qquad \left.\left. + O\big(\xi_{-i}^2\big)\right)\right\rangle \\
&= \frac{\bar{k}_i}{\bar{k}_{-i}} \left\langle 1 + \xi_i\,\eta_i(t) - \xi_{-i}\,\eta_{-i}(t) \right. \\
&\qquad \left. - \xi_{-i}\xi_i\,\eta_{-i}(t)\,\eta_i(t) + O\big(\xi_{-i}^2\big) \right\rangle \\
&= \frac{\bar{k}_i}{\bar{k}_{-i}} \left(1 + \xi_{-i}^2\right) = K_i^{\mathrm{eq}}\big(1 + \xi_{-i}^2\big). \tag{13}
\end{aligned}
$$

Thus the average of the fluctuating equilibrium constant for the ith reversible reaction is equal to the deterministic equilibrium constant up to corrections of *second order* in the noise amplitude for the inverse reaction. For small noise amplitudes, these second order corrections are negligible compared to unity. So, for example, for two independent processes which have identical deterministic equilibrium constants (e.g., the direct production d of enantiomers and enantioselective autocatalysis a), thus $K_d^{\mathrm{eq}} = K_a^{\mathrm{eq}}$, and then the temporal average implies

$$\langle K_d^{\mathrm{eq}}(t) \rangle = \langle K_a^{\mathrm{eq}}(t) \rangle + K_d^{\mathrm{eq}}\big(\xi_{-d}^2 - \xi_{-a}^2\big). \tag{14}$$

The averaged equilibrium constants are equal up to corrections of second order in the noise amplitudes for the associated inverse processes. Thus T fluctuations do break the detailed balance constraint $K_d^{\mathrm{eq}} = K_a^{\mathrm{eq}}$, although the amount of breaking is minuscule.

IV. AN OPEN-FLOW STOCHASTIC FRANK MODEL

We consider a simple open-flow and fully reversible version of the Frank model [20] for analyzing the competition between the temperature fluctuations and the deterministic chiral bias (PVED). These fluctuations and bias directly affect the rate constants. It is worth remarking that, apart from playing a privileged role in the modeling of spontaneous mirror symmetry breaking in chemistry, nowadays the rationalizations of the Soai reaction [12–15] all consider a reaction network similar to that of Frank's original proposal, namely, first order autocatalysis coupled to a heterochiral reaction coupling, known as the mutual inhibition step. In these more elaborate and extended kinetic models, the enantioselective autocatalysis and mutual inhibition are provided by the involvement of oligomeric intermediates. Moreover, the thermodynamic scenario for spontaneous mirror symmetry breaking (SMSB) is that of nonequilibrium thermodynamics.

In the fully reversible Frank model in an open flow reactor of volume V, an achiral species A flows in at constant concentration $[A]_{\mathrm{in}}$, and all species A, L, D, and P flow out with
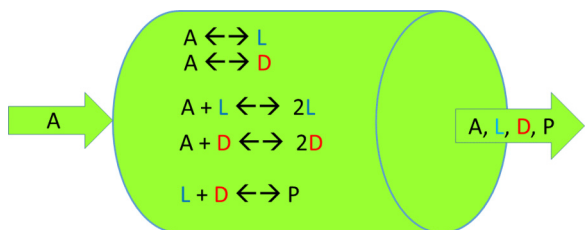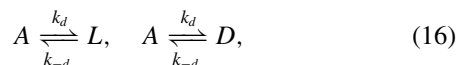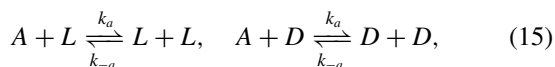
FIG. 1. Reversible version of the Frank model in a continuous open-flow reactor of volume V at *mean* temperature T, assuming instant and perfect diffusion of all the species in solution. Achiral resource A flows in at fixed concentration $[A]_{in}$; all species A, L, D, and P flow out with their instantaneous concentrations. The matter flow maintains the system out of chemical equilibrium. The fluid volumes entering and exiting the reactor per unit time are the same.

their instantaneous concentrations according to the following transformations (see Fig. 1):

$$A + L \underset{k_{-a}}{\overset{k_a}{\rightleftharpoons}} L + L, \quad A + D \underset{k_{-a}}{\overset{k_a}{\rightleftharpoons}} D + D, \tag{15}$$

$$A \underset{k_{-d}}{\overset{k_d}{\rightleftharpoons}} L, \quad A \underset{k_{-d}}{\overset{k_d}{\rightleftharpoons}} D, \tag{16}$$

$$L + D \underset{k_{-1}}{\overset{k_1}{\rightleftharpoons}} P, \tag{17}$$

$$\bar{\emptyset} \xrightarrow{k_f [A]_{in}} A, \tag{18}$$

$$A \xrightarrow{k_f} \emptyset, \tag{19}$$

$$L \xrightarrow{k_f} \emptyset, \tag{20}$$

$$D \xrightarrow{k_f} \emptyset, \tag{21}$$

$$P \xrightarrow{k_f} \emptyset, \tag{22}$$

where $k_f = q/V$, the volumetric flow rate q is in liters per second, and V is in liters. Equality of the deterministic equilibrium constants for the direct production (16) and the autocatalytic steps (15) implies the constraint for the reaction rate constants [21], and for the associated equilibrium constants [22]:

$$\frac{k_a}{k_{-a}} = \frac{k_d}{k_{-d}}. \tag{23}$$

These transformations [Eqs. (15)–(22)] lead to the following set of differential rate equations for the concentrations:

$$\frac{d[A]}{dt} = -2k_d[A] + k_{-d}([D] + [L]) - k_a[A]([L] + [D]) + k_{-a}([L]^2 + [D]^2) + k_f([A]_{in} - [A]), \tag{24}$$

$$\frac{d[L]}{dt} = k_d[A] - k_{-d}[L] + k_a[A][L] - k_{-a}[L]^2 - k_1[L][D] + k_{-1}[P] - k_f[L], \tag{25}$$

$$\frac{d[D]}{dt} = k_d[A] - k_{-d}[D] + k_a[A][D] - k_{-a}[D]^2 - k_1[L][D] + k_{-1}[P] - k_f[D], \tag{26}$$

$$\frac{d[P]}{dt} = k_1[L][D] - k_{-1}[P] - k_f[P]. \tag{27}$$

These imply the constraint

$$\frac{d}{dt}([A] + [L] + [D] + 2[P]) = k_f([A]_{in} - [A] - [L] - [D] - 2[P]), \tag{28}$$

and in the steady state the total chemical mass in the reactor is equal to the input mass $[A]_{in}$:

$$[A]_{in} = [A] + [L] + [D] + 2[P]. \tag{29}$$

We next write down the stochastic version of Eqs. (24)–(27), by writing those in terms of the fluctuating rate constants [Eq. (10)]. This yields the following set of stochastic differential rate equations subject to multiplicative noise:

$$\frac{d[A]}{dt} = -k_d(1 + \xi_{dL}\eta_{dL}(t))[A] + k_{-d}(1 + \xi_{-dL}\eta_{-dL}(t))[L] - k_a(1 + \xi_{aL}\eta_{aL}(t))[A][L] + k_{-a}(1 + \xi_{-aL}\eta_{-aL}(t))[L]^2$$
$$- k_d(1 + \xi_{dD}\eta_{dD}(t))[A] + k_{-d}(1 + \xi_{-dD}\eta_{-dD}(t))[D] - k_a(1 + \xi_{aD}\eta_{aD}(t))[A][D] + k_{-a}(1 + \xi_{-aD}\eta_{-aD}(t))[D]^2$$
$$+ k_f([A]_{in} - [A]), \tag{30}$$

$$\frac{d[L]}{dt} = k_d(1 + \xi_{dL}\eta_{dL}(t))[A] - k_{-d}(1 + \xi_{-dL}\eta_{-dL}(t))[L] + k_a(1 + \xi_{aL}\eta_{aL}(t))[A][L] - k_{-a}(1 + \xi_{-aL}\eta_{-aL}(t))[L]^2$$
$$- k_1(1 + \xi_1\eta_1(t))[L][D] + k_{-1}(1 + \xi_{-1}\eta_{-1}(t))[P] - k_f[L], \tag{31}$$

$$\frac{d[D]}{dt} = k_d(1 + \xi_{dD}\eta_{dD}(t))[A] - k_{-d}(1 + \xi_{-dD}\eta_{-dD}(t))[D] + k_a(1 + \xi_{aD}\eta_{aD}(t))[A][D] - k_{-a}(1 + \xi_{-aD}\eta_{-aD}(t))[D]^2$$
$$- k_1(1 + \xi_1\eta_1(t))[L][D] + k_{-1}(1 + \xi_{-1}\eta_{-1}(t))[P] - k_f[D], \tag{32}$$

$$\frac{d[P]}{dt} = k_1(1 + \xi_1\eta_1(t))[L][D] - k_{-1}(1 + \xi_{-1}\eta_{-1}(t))[P] - k_f[P]. \tag{33}$$

Note there are ten *independent* one-way (forward and reverse) reactions in Eqs. (15)–(17), so we must allow for the same number of independent noise terms $\eta_j(t)$, each one being multiplied by a corresponding amplitude ξ_j [23], and $\Delta H_j^{\ddagger} > 0$ is the activation enthalpy of the jth reaction [see Eq. (9) in Sec. II A]:

$$\xi_j = \frac{\Delta H_j^{\ddagger}}{RT}\sqrt{\frac{k_B}{C_V}} > 0. \tag{34}$$

The fluid flow rate k_f does not depend on the temperature, consequently we take it as a fixed parameter. We verify that the total mass constraint [Eq. (C7)] continues to hold in the presence of fluctuations.

Regarding the thermodynamic constraint [see Eqs. (14) and (23)], this is given by

$$\langle K_a^{\text{eq}}(t)\rangle = \langle K_d^{\text{eq}}(t)\rangle\left(1 + \xi_{-a}^2 - \xi_{-d}^2\right), \tag{35}$$

indicating that the averages of the (fluctuating) equilibrium constants for the direct production (d) and the autocatalysis (a) are equal up to corrections of *second order* in the temperature induced fluctuations of the reverse reactions (see Sec. III).

V. PVED SELECTIVITY CRITERION

To investigate the competition between the deterministic PVED chiral polarization and thermal noise, we first estimate some numbers. The current theoretical estimates for the transition state energy difference between enantiomeric molecules are on the order of $\Delta\Delta G^{\ddagger}|_{300K} = 10^{-13}$–$10^{-20}$eV at room temperature [24]. The constants and conversion factors needed to convert eV to J and then to J/mol are

$$R = 8.314\,\text{J mol}^{-1}\,\text{K}^{-1}, \tag{36}$$

$$N_A = 6.022 \times 10^{23}\,\text{mol}^{-1}, \tag{37}$$

$$1\,\text{eV} = 1.602 \times 10^{-19}\,\text{J} \tag{38}$$

$$\Rightarrow 1\,\text{eV} = 9.648 \times 10^4\,\text{J/mol}. \tag{39}$$

Hence, using the estimated upper bound we obtain

$$\Delta\Delta G^{\ddagger}|_{300\,\text{K}} = 10^{-13}\,\text{eV} \tag{40}$$

$$= 10^{-13}\,\text{eV} \times \left(\frac{9.65 \times 10^4\,\text{J/mol}}{\text{eV}}\right) \tag{41}$$

$$= 9.65 \times 10^{-9}\,\text{J/mol} \tag{42}$$

$$\simeq 10^{-8}\,\text{J/mol}, \tag{43}$$

$$\frac{\Delta\Delta G^{\ddagger}}{RT}\Big|_{300\,\text{K}} = \frac{10^{-8}\,\text{J/mol}}{2.5 \times 10^3\,\text{J/mol}} = 4.0 \times 10^{-12}. \tag{44}$$

Chiral bias explicitly breaks the $L \leftrightarrow D$ symmetry in the rate constants for the autocatalysis and direct production, so we need to distinguish this fact in the transformations involving only the L enantiomer from those involving only the D. To do so, we write k_{aL}, k_{-aL} on the left hand side of Eq. (15) (and k_{aD}, k_{-aD} on the right), and write k_{dL}, k_{-dL} on the left hand

of Eq. (16) (and k_{dD}, k_{-dD} on the right), keeping all other rate constants and flow terms unchanged.

Now the ratio of the forward rate constants $k_{aL} \neq k_{aD}$ for the enantioselective autocatalysis [see Eq. (15)] is then given by (and for the upper bound estimate)

$$\frac{k_{aL}}{k_{aD}} = \exp\left(-\frac{\Delta\Delta G^{\ddagger}}{RT}\right) \tag{45}$$

$$\simeq 1 - 10^{-12} = (1 - g). \tag{46}$$

From Fig. 2 we quantify the direct production in terms of the PVED energy difference as follows. A reasonable approximation is $k_{dL} = k_{dD}$ for the forward rate constants, but with $k_{-dL} < k_{-dD}$ for the inverse ones (see top right in Fig. 2). It then follows that

$$k_{-dL} = \exp\left(-\frac{\Delta\Delta G^{\ddagger}}{RT}\right)k_{-dD} \tag{47}$$

$$\Rightarrow \frac{k_{dL}}{k_{-dL}} = \exp\left(+\frac{\Delta\Delta G^{\ddagger}}{RT}\right)\frac{k_{dD}}{k_{-dD}} \tag{48}$$

$$\Rightarrow K_L^d > K_D^d, \tag{49}$$

the final inequality holding for the equilibrium constants for the direct production of the enantiomers. Next, we assume equality between the equilibrium constants for autocatalysis
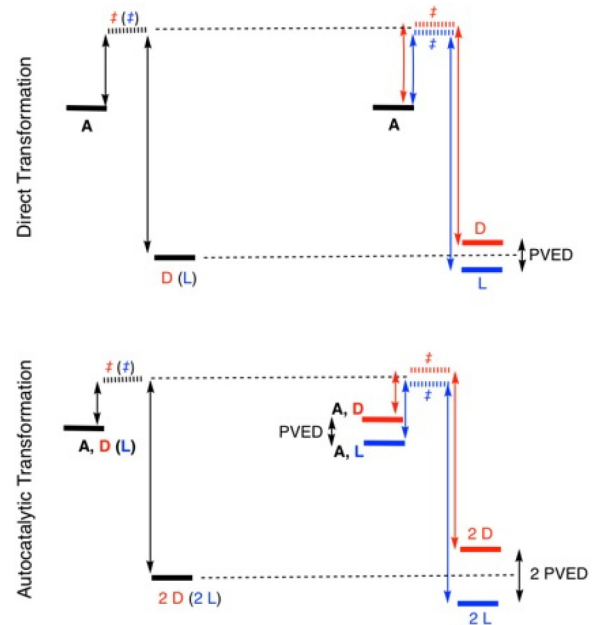

FIG. 2. Reaction coordinate diagrams corresponding to the noncatalytic or spontaneous (top) and the autocatalytic (bottom) reactions, respectively. Left: Reactants, transition states ($\ddagger$), and products in the absence of PVED. Right: The effect of the PVED on the energies of the individual enantiomers L and D and the transition states. These (minuscule) energy differences $\Delta\Delta G^{\ddagger} > 0$ in the enantiomers appear only in those processes involving the enantiomers.

(K^a) and direct production (K^d) for each enantiomer *separately* [see also Eq. (23)]:

$$K_L^a = K_L^d, \qquad K_D^a = K_D^d, \tag{50}$$

$$\Rightarrow K_L^a = \exp\left(+\frac{\Delta\Delta G^{\ddagger}}{RT}\right)K_D^a, \tag{51}$$

where the second line follows immediately from Eqs. (48) and (50). We parametrize the relation between the forward (and also the reverse) rate constants for the enantioselective autocatalyses as follows:

$$k_{aL} = \exp\left(a\frac{\Delta\Delta G^{\ddagger}}{RT}\right)k_{aD} \tag{52}$$

$$k_{-aL} = \exp\left(b\frac{\Delta\Delta G^{\ddagger}}{RT}\right)k_{-aD} \tag{53}$$

$$\Rightarrow \frac{k_{aL}}{k_{-aL}} = \exp\left((a-b)\frac{\Delta\Delta G^{\ddagger}}{RT}\right)\frac{k_{aD}}{k_{-aD}}, \tag{54}$$

where we must have $a - b = 1$ according to Eq. (51), whereas from the diagram in Fig. 2 we have $|a| = 1$, $|b| = 2$. The unique solution is $a = -1$ and $b = -2$. Thus, $k_{aL} < k_{aD}$ and $k_{-aL} < k_{-aD}$, and we have $K_L^a = K_L^d > K_D^a = K_D^d$, in accord with Eqs. (49) and (50).

Considering the current range of theoretical predictions for the energy difference between enantiomeric molecules, the above calculations imply, e.g., that

$$\frac{k_{aL}}{k_{aD}} = 1 - 10^{-12,-19} = (1-g), \tag{55}$$

and define the range of the dimensionless parameter $10^{-19} \lesssim g \lesssim 10^{-12}$, which provides a measure of the chiral bias.

So, to include chiral bias in the (stochastic) rate equations we make the following substitutions in the first two rate equations [Eqs. (30) and (31)], and only in the terms that contain $[L]$, but in no term containing $[D]$ (resulting in three substitutions):

$$k_{-d} \rightarrow (1-g)k_{-d}, \tag{56}$$

$$k_a \rightarrow (1-g)k_a, \tag{57}$$

$$k_{-a} \rightarrow (1-2g)k_{-a}. \tag{58}$$

From Eqs. (3) and (8) for $\delta_T k = k(T \pm \delta T) - k(T)$ and Eq. (55), we estimate the relative magnitude of the time dependent fluctuations induced in the ith rate constant by the temperature fluctuations,

$$\frac{\delta_T k_i}{k_i} \simeq \frac{\Delta H_i^{\ddagger}}{RT}\left(\frac{\delta T}{T}\right)_{\text{rms}} = \frac{\Delta H_i^{\ddagger}}{RT}\sqrt{\frac{k_B}{C_V}}, \tag{59}$$

and that corresponding to the constant PVED bias g is

$$\frac{\delta_{\text{PVED}}(k_L - k_D)_i}{(k_D)_i} = g. \tag{60}$$

These considerations point to the following selectivity criterion. That is, when the PVED bias in the rate constant for the ith transformation is greater than the fluctuations induced in

that rate constant by the ambient rms temperature fluctuations (in absolute values),

$$\frac{\delta_{\text{PVED}}(k_L - k_D)_i}{(k_D)_i} \gtrsim \frac{\delta_T k_i}{k_i}, \tag{61}$$

$$g = \frac{\Delta\Delta G_i^{\ddagger}}{RT} \gtrsim \frac{\Delta H_i^{\ddagger}}{RT}\sqrt{\frac{k_B}{C_V}} = \xi_i, \tag{62}$$

then we might rightfully expect that the chiral bias g can overcome the thermal noise ξ_i, and therefore *selects* the final stable chiral outcome, provided the inequality $g > \xi_i$ holds for all the reactions i in which the bias intervenes. This is also an order-of-magnitude estimate of the energy of interaction $\Delta\Delta G_i^{\ddagger}$ required to produce a macroscopic chiral selection. This condition [Eq. (62)] can be cast as follows:

$$\frac{\Delta\Delta G_i^{\ddagger}}{\Delta H_i^{\ddagger}} \gtrsim \sqrt{\frac{k_B}{C_V}}. \tag{63}$$

The left hand side of Eq. (63) is *independent of the temperature*; it depends on the ratio of the PVED energy difference to the activation enthalpy between transition state and reactants (or products) for reaction i. The right hand side depends on the temperature through the constant volume heat capacity $C_V(T)$, and is *universal*, in that it is independent of the specific reaction i. According to this criterion, systems composed of otherwise mirror-symmetric reactions and with sufficiently large heat capacity C_V would have their net chirality sign selected by the deterministic PVED bias, provided of course there were no other sources of chiral bias.

Our selectivity criterion, Eqs. (61)–(63), is radically different from the one derived decades ago by Kondepudi and Nelson [7,8]. Using bifurcation theory, those authors arrived at the criterion

$$g > \left(\frac{8}{27}\right)\left(\frac{U}{4W}\right)\langle\alpha^2\rangle^{3/2}, \tag{64}$$

where $\alpha = ([L] - [D])/2$ and U and W are specific functions of the model parameters (rate constants, external clamped concentrations, etc). For these model dependent prefactors, Eq. (64) states that the chiral bias g must be greater than the *cube* of the rms chiral fluctuation in the composition, $\langle\alpha^2\rangle^{1/2}$, and this inequality must hold at the critical point of the bifurcation, where the distance between the upper and lower stable scalemic branches is a minimum (see Appendix D). This criterion also envisaged that the chemical system could migrate or evolve starting off on the single stable scalemic branch below the critical point, and then pass through the critical point under the variation of an externally controllable parameter. The inequality is the condition for the system to remain on the *same* scalemic branch that it starts off on as it evolves under the variation of an external parameter.

Our criterion Eq. (62) states that for the chiral bias to be a good selector, it should be greater in magnitude than the relative rms temperature fluctuations times a factor proportional to the activation enthalpy for the ith reaction. We also consider the system to be located initially on a nonequilibrium racemic configuration (which in the presence of bias is never *stationary*), typically above the critical point, without having had to *evolve* there via the variation or tuning of any external
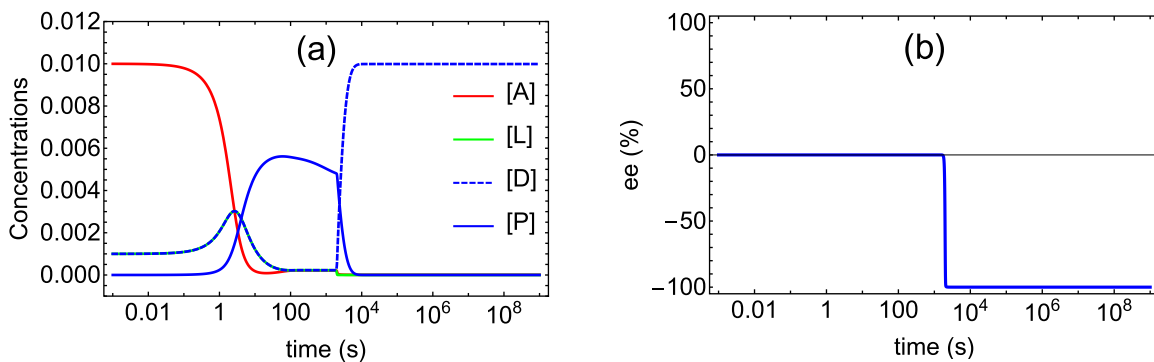
FIG. 3. Characteristic dynamic outcome of deterministic mirror symmetry breaking triggered by a minuscule PVED bias $g = 10^{-19}$ [Eq. (55)], in the *absence* of all fluctuations, for the open flow Frank model (see Sec. IV). (a) The evolution of all four chemical species. (b) The percent of enantiomeric excess ee(%) = ([L] − [D]/[L] + [D]) × 100. The outcome is homochiral in favor of the D enantiomer. Changing the *sign* of the PVED bias to $g = -10^{-19}$ leads to the opposite homochiral outcome, now in favor of the L (not shown). See text for related comments, the parameter values employed, and also Fig. 7 in Appendix D for a characteristic imperfect (biased) bifurcation.

parameter. Thus, in the absence of fluctuations, the system would evolve deterministically to the preferred final scalemic state, because the racemic configuration lies inside the basin of attraction of the preferred stable scalemic branch (see Fig. 7 in Appendix D).

But sufficiently large temperature fluctuations could well take the system out of that basin into the basin of attraction belonging to the *other* stable scalemic branch. These two basins of attraction are separated by an unstable *scalemic* branch that lies close to the horizontal axis of racemic configurations (see Fig. 7 in Appendix D).

The selectivity criterion Eq. (62) is a condition for each individual rate constant, but not all the rate constants in a model that can undergo SMSB will necessarily depend on a bias, as, for example, in achiral transformations such as mutual inhibition and heterodimer decay into enantiomers [Eq. (17)]. For such achiral transformations, Eq. (62) cannot apply since $g = 0$ for those processes (the transition state is achiral). Thus the selectivity could be absolute (deterministic) or partial (statistical); we will see examples of these kinds of selectivity in the next section.

VI. RESULTS

For the numerical simulations we generate uniformly distributed random numbers lying in the range $-1 \leqslant x \leqslant 1$, and then use INTERPOLATINGFUNCTION to build continuous time-dependent noise functions $\eta(t)$ based on these random number sets. The time resolution in these noise functions is chosen to be equal to the time step Δt used in the simulations. From Eq. (10) this then implies that the relative rate constant fluctuations lie in the range $(-\xi, \xi)$, which involve rms temperature fluctuations within one standard deviation from the mean value [Eq. (7)]. The stochastic differential equations are integrated numerically using the MATHEMATICA function NDSOLVE with options MAXSTEPS→ 10^6 and WORKINGPRECISION→ 30. All the initial conditions and parameters are specified with SETPRECISION set to 30. The outputs using INTERPOLATINGFUNCTION are used to evaluate the dynamics, the enantiomeric excesses, etc.

Our goal is to focus on the competition between the deterministic PVED bias g and the random temperature fluctuations ξ in the reaction rate constants, and when the system is initially situated on a nonequilibrium racemic configuration. Before dealing with this, we first must ensure that, in the absence of all fluctuations (including computational noise from roundoff error) and biases, the system remains on the unstable racemic branch (see Fig. 7 in Appendix D) during the full temporal range of the simulations, from $t = 0$ to 10^{20} s, which is more than sufficient for our purposes (the age of the Universe is on the order of 10^{17} s). This is achieved by working with a sufficiently high numerical precision.

Moreover, as we are dealing with both extremely tiny PVED biases g and minuscule temperature fluctuations ξ, on orders of magnitude as small as 10^{-20}, we need to employ an adequate numerical precision in order that such small numbers are to remain significant during the full duration of the simulations, and not be lost in numerical roundoff errors [25]. Hence in our simulations, we have set all model parameters and initial conditions up to 40 digit working precision, and the numerical integration scheme (NDSOLVE) employs a working precision of 33 digits, respectively. This affords an ample and safe margin in our calculations. Then we have confirmed that, in the absence of bias and fluctuations, strictly racemic initial conditions lead to a racemic outcome, and during the full temporal range employed in all the simulations.

We first consider the effect of a minuscule bias $g = 10^{-19}$ in the reaction rate constants [Eqs. (56)–(58)] (and zero fluctuations and noise) following Sec. V, which corresponds to the current minimum theoretical estimate of the PVED [24]. Set all the $\xi_i = 0$. The results are shown in Fig. 3. The system experiences an imperfect deterministic bifurcation from an initially racemic composition, or mirror-symmetric state, to the preferred stable scalemic (it is enantiomerically pure) branch selected by the sign of $g > 0$. There is a relatively short induction period in which both the enantiomers L and D remain close to their initial concentrations, followed by a burst in their joint concentrations and corresponding consumption of the achiral resource A. This is followed by a rapid increase in the production of the achiral heterodimer P, with a corresponding drop in the still joint concentrations of L and D
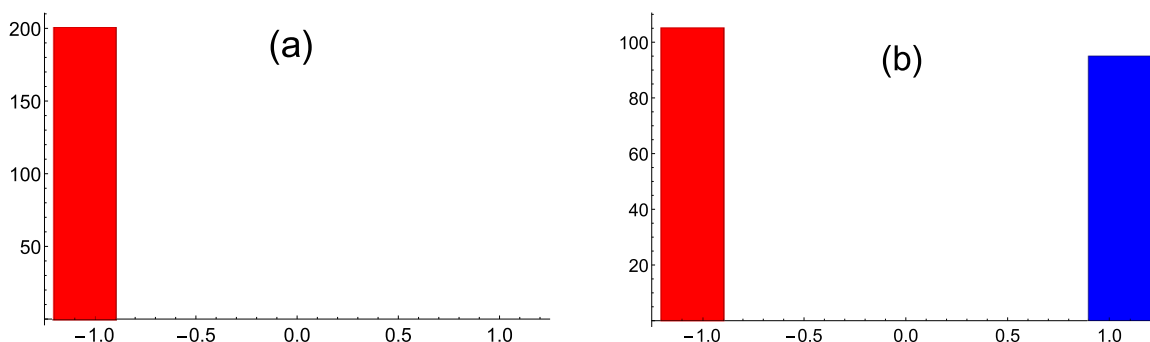
FIG. 4. Distributions of the outcomes from multiple simulations $n = 200$ of the reaction model. (a) Subject exclusively to chiral bias $g = 10^{-19}$ and zero fluctuations $\xi = 0$. (b) Subject to pure thermal fluctuations $\xi = 10^{-22}$ and in the absence of any chiral bias $g = 0$. The red (blue) column corresponds to total number of final homochiral D (L) states. See text for related comments and Fig. 7 in Appendix D for a structure of imperfect and perfect bifurcations.

to a level even lower than their initial conditions. The high level of heterodimer and the low levels of the enantiomers become jointly unstable, provoking the biased bifurcation in the enantiomeric concentrations along with a dramatic drop in the heterodimer concentration, and an increase in the favored enantiomer (in this case, it is the D). Here, the heterodimer P gets depleted by virtue of the inverse reaction [Eq. (17)], and dissociates back into the individual enantiomers. Beyond the symmetry breaking transition point, the system remains in this stable chiral NESS for as long as the fluid flow, supplying the fixed concentration of achiral molecule A to the reactor [Eq. (18)], is maintained. Here we show the details of the mirror symmetry breaking transition by plotting the results in the temporal window 10^{-3} s $\leqslant t \leqslant 10^{9}$ s (see Fig. 3).

The reaction model subject exclusively to a minuscule chiral bias ($g = 10^{-19}$) and no fluctuations always ends up in the same final stable homochiral D state. This single outcome is selected deterministically by the sign of the chiral bias, and for an arbitrary number of repetitions or trials. This results in a unimodal distribution [Fig. 4(a)]. In marked contrast, the same system subject to minuscule thermal fluctuations on the order of $\xi = 10^{-22}$ and zero bias ($g = 0$) leads instead to a stochastic and bimodal distribution of outcomes [see Fig. 4(b)]. The evolution of the system under temperature fluctuations alone and for multiple runs shows that the symmetry breaking can occur at different times (see Fig. 8 in Appendix E).

We now consider the dynamics of the model in the presence of *both* temperature fluctuations (see Sec. IV) and the PVED (Sec. V). We begin by assessing the competition between the current estimated upper bound on the PVED, $g = 10^{-12}$, and the rate constant fluctuations (induced by the temperature fluctuations) for various orders of magnitude ranging from below to above the PVED bias. The model parameters are taken to be as follows: $k_d = 10^{-4}$, $k_{-d} = 10^{-9}$, $k_a = 10^{2}$, $k_{-a} = 10^{-3}$, $k_1 = 10^{2}$, $k_{-1} = 10^{-4}$, $[A]_{\text{in}} = 10^{-2}$, and the flow rate $k_f = 10^{-3}$. We initiate all the simulations on the racemic composition: $[L]_0 = [D]_0 = 10^{-3}$, with $[P]_0 = 10^{-6}$ and $[A]_0 = [A]_{\text{in}}$. Recall, moreover, that each effective noise amplitude ξ_j results from the product of the activation enthalpy factor for the jth reaction, multiplied by the rms temperature fluctuation [Eq. (34)]. The former depends on the energetics of the specific chemical transformation, whereas the latter is universal, being a physical property of

the medium, namely, its heat capacity at constant volume. For simplicity, we take all $\xi_j = \xi$ amplitudes to be the same, actually a reasonable approximation since the activation energies $\frac{\Delta G_i^{\ddagger}}{RT}$ are all of the *same order of magnitude* as implied by the model's rate constants (see middle column of Table I).

We carry out a series of n runs. A set of outcomes is shown in Fig. 5. Depending on the relative values of g and ξ each individual run $1 \leqslant j \leqslant n$ will give rise to a dynamic result qualitatively identical to that in Fig. 3, where either the L or the D enantiomer is the majority (actually, 100% homochiral). We then collect the output of all the n runs in two bins: one for ee $= -1$, the other for ee $= +1$. Depending on the level of the noise amplitude ξ, the final stationary outcomes are either unimodal (deterministic) or bimodal (stochastic), and the latter may exhibit a significant asymmetric bias induced by PVED. Figure 5(a) shows the outcome for $n = 60$ trials using the noise amplitude $\xi = 10^{-13}$, ten times *smaller* that the PVED value. The resultant unimodal distributions indicate that the PVED is still an efficient selector of the final chiral sign. This case is not unexpected as the thermal fluctuations are smaller than the PVED. In Fig. 5(b), the noise amplitude $\xi = 10^{-12}$ is now further increased to be of the *same* order as the PVED. Surprisingly, for this case the PVED continues to act as an efficient selector of the final chiral sign, and the outcomes, also for $n = 60$ trials, are still unimodal (deterministic). This case is more interesting as it shows a certain resilience to the noise. If we now increase the noise level to $\xi = 10^{-11}$, an order of magnitude greater than the PVED, and for $n = 120$ trials, the outcomes are bimodal (stochastic), albeit indicating a significant bias for the preferred enantiomer induced by the PVED [see Fig. 5(c)]. Here, we are at the competition point; this is the bias which is the key point. Finally, increasing the noise level yet further to $\xi = 10^{-10}$, now two orders of magnitude greater than the PVED bias, and for $n = 60$ trials, the outcomes are bimodal (stochastic) and without indicating any statistically significant preference for either enantiomer [see Fig. 5(d)]. The PVED bias is washed out by the noise.

We next carry out a series of simulations employing $g = 10^{-17}$, now five orders of magnitude smaller than the previous value. The results are shown in Fig. 6, and all for $n = 120$ independent runs, in varying the noise amplitude from $\xi = 10^{-18}$ to 10^{-15}, ranging from an order of magnitude
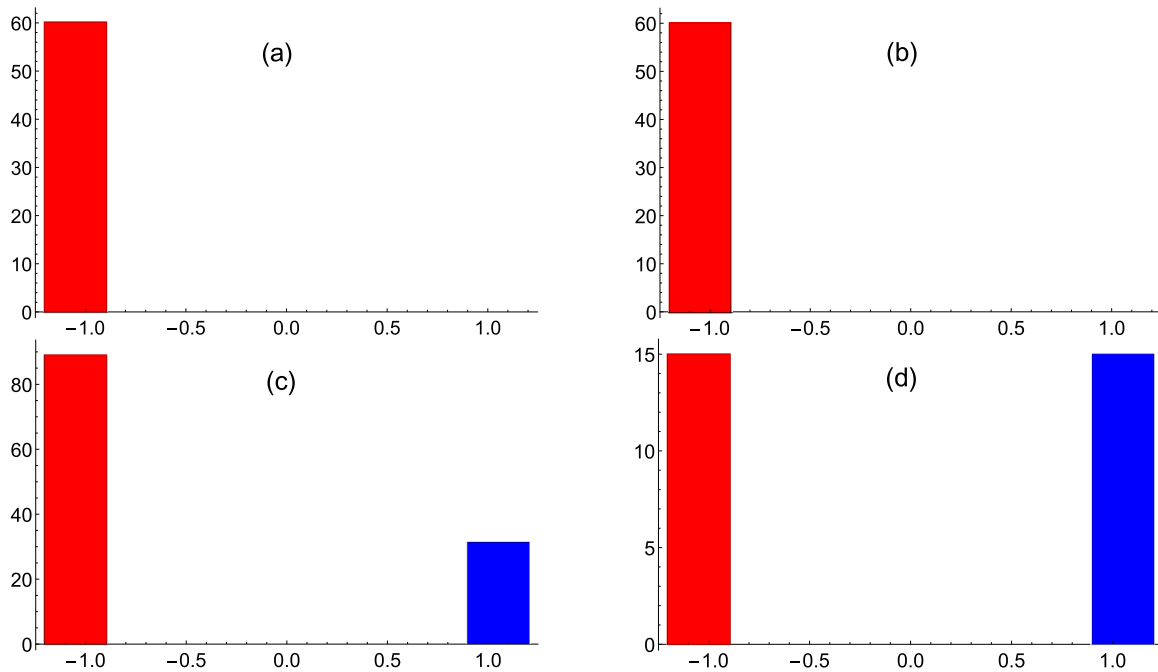
FIG. 5. Distributions of the outcome from multiple simulations n of the competition between the PVED [Eq. (55)] and the product of the rms temperature fluctuation times the activation enthalpy factor ξ_j [Eq. (34)]. The level of chiral bias corresponds to $g = 10^{-12}$. (a) $\xi = 10^{-13}$ and $n = 60$. (b) $\xi = 10^{-12}$ and $n = 60$. (c) $\xi = 10^{-11}$ and $n = 120$. (d) $\xi = 10^{-10}$ and $n = 30$. The red (blue) bar centered at -1 ($+1$) represents the total number of stationary homochiral outcomes for which the final majority enantiomer is D or L. See text for related comments.

smaller up to two orders of magnitude greater than the PVED bias. In contrast to the previous case, the now much smaller value of g fails to act as a deterministic selector of the final chiral sign even for noise levels an order of magnitude

smaller [Fig. 6(a)], and also for noise levels of the same order [Fig. 6(b)], since the distributions of the homochiral outcomes are bimodal, albeit showing significant bias for the preferred enantiomer. For thermal noises an order of magnitude greater,
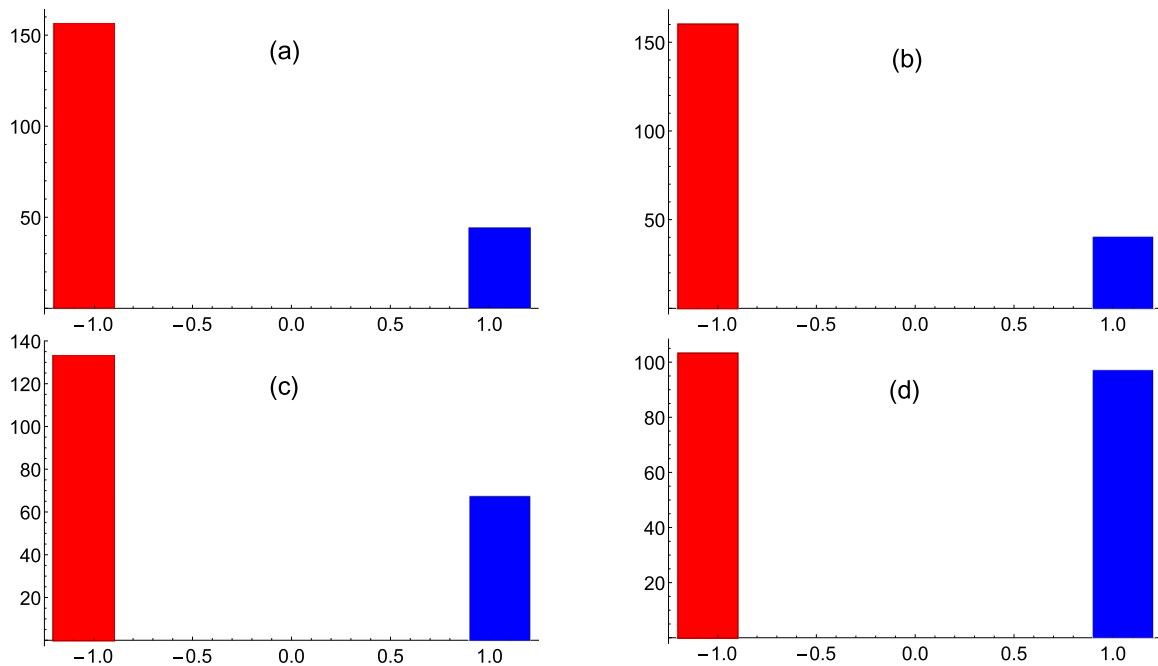

FIG. 6. Distributions of the outcome from multiple simulations $n = 200$ of the competition between the PVED [Eq. (55)] and the product of the rms temperature fluctuation times activation enthalpy factor ξ_j [Eq. (34)]. Chiral bias corresponds to $g = 10^{-17}$. (a) $\xi = 10^{-18}$. (b) $\xi = 10^{-17}$. (c) $\xi = 10^{-16}$. (d) $\xi = 10^{-15}$. The red (blue) bar centered at -1 ($+1$) represents the total number of stationary homochiral outcomes for which the final majority enantiomer is D or L. See text for further remarks.

$\xi = 10^{-16}$, the PVED bias is still significant [Fig. 6(c)]. But for noise amplitudes $\xi = 10^{-15}$ now two orders of magnitude greater than the PVED, the chiral bias is lost and we recover a bimodal distribution, statistically indistinguishable from the case of unbiased equally likely random outcomes [Fig. 6(d)].

Finally, we recall that, in the absence of noise $\xi = 0$, a PVED bias as small as $g = 10^{-19}$ is still a deterministic selector of the outcome [see Fig. 4(a)]. However, even for noise amplitudes two to three orders of magnitude smaller than this bias $\xi \ll 10^{-19}$, the outcomes are statistically indistinguishable from the unbiased random case (i.e., an ideal "coin toss"), qualitatively similar to the outcomes in, for example, Figs. 5(d) and 6(d). Thus, a $g = 10^{-19}$ is probably already a value smaller than the lower bound on the PVED bias that can be amplified in the presence of thermal noise.

VII. PVED DETECTOR

We can estimate the order-of-magnitude size for the minimum reactor volumes such that the product of the rms temperature fluctuations [Eq. (7)] times the transition enthalpy factor [Eq. (9)] for the reaction is less than the value of the PVED bias g, in accord with our selectivity criterion Eq. (62).

To do so, we evaluate C_V for a volume filled with water (solvent). Consider first a reactor of length scale, or characteristic size, of 1 cm $= 10^{-2}$ m. The specific constant volume heat capacity for H_2O at room temperature is 4.18 MJ/m^3 K. The corresponding constant volume heat capacity for this reactor is then

$$C_V = 4.18 \times 10^6 \text{ J/m}^3 \text{ K} \times (10^{-2} \text{ m})^3 = 4.18 \text{ J/K}. \quad (65)$$

Now the Boltzmann constant $k_B = 1.380\,66 \times 10^{-23}$ J K^{-1}, so that from Eq. (7) we have

$$\frac{\delta T_{\text{rms}}}{T} = \sqrt{\frac{k_B}{C_V}} = \frac{3.71 \times 10^{-12} \sqrt{\text{J/K}}}{\sqrt{C_V}} \quad (66)$$

$$= \frac{3.71 \times 10^{-12}}{\sqrt{4.18}} = 1.82 \times 10^{-12}. \quad (67)$$

Then from Eqs. (7) and (9), the amplitude of the fluctuation in a reaction rate constant is

$$\xi = \frac{\Delta H^{\ddagger}}{RT} \sqrt{\frac{k_B}{C_V}} = \frac{\Delta H^{\ddagger}}{RT} (1.82 \times 10^{-12}). \quad (68)$$

The overall magnitude depends on the specific energetics of the reaction. Assuming, by way of example, that the transition enthalpy lies in the range $10 \leqslant \frac{\Delta H^{\ddagger}}{RT} \leqslant 100$, then

$$10^{-11} \leqslant \xi \leqslant 10^{-10}, \quad (69)$$

so that a PVED bias of the order of $g \gtrsim 10^{-11}, 10^{-10}$ might be detectable, with Eq. (62) holding for all reactions involving the enantiomers.

For a reactor of linear size of 10 cm $= 10^{-1}$ m, then the numbers work out to give

$$\xi = \frac{\Delta H^{\ddagger}}{RT} \sqrt{\frac{k_B}{C_V}} = \frac{\Delta H^{\ddagger}}{RT} (5.8 \times 10^{-14}), \quad (70)$$

so that fluctuations on the reaction rate constant lie in the range

$$10^{-13} \leqslant \xi \leqslant 10^{-12}, \quad (71)$$

and a homogeneous reactor of this size scale might be able to detect a PVED bias on the order of $g = 10^{-12}, 10^{-13}$, for example. These are both very small, laboratory-size reactors such as those used in modern microfluidic techniques.

Given the optimal sizes, the spatial homogeneity of the reactants is desired to suppress concentration gradients and so reaction noise, due to fluctuations in the numbers of species. This means we want to operate these reactors in the regime of the thermodynamic limit. Recall, the thermodynamic limit corresponds to the infinite-population, infinite-volume, finite-concentration limit in which the stochastic chemical Langevin equation (CLE) reduces to the deterministic reaction rate equations [26]. As the thermodynamic limit is approached, the deterministic terms on the left side of the CLE grow like the system size, whereas the noise terms grow more slowly, and as the square root of the system size. In the full thermodynamic limit, the reaction noise terms becomes negligibly small compared with the deterministic terms.

Note, in the case of temperature fluctuations, the stochastic noise terms in Eqs. (30)–(33) are directly proportional to the reaction rates themselves, and not their square roots, as is the case of the CLE for reaction noise.

VIII. CONCLUDING REMARKS

In this paper we have shown that the characteristic amplitude of the relative fluctuation $\delta k_i / k_i$ in the ith reaction rate constant, driven by nonequilibrium temperature fluctuations, is given by the product of two distinct contributions, namely, (i) the activation enthalpy of the reaction (divided by RT) multiplied by (ii) a thermodynamic factor proportional to the inverse square root of the heat capacity at constant volume [Eq. (4)]. The former is specific to the individual reaction energetics, whereas the latter is a property of the material composition of the bulk solvent or medium in which the reaction can take place. This amplitude expression Eq. (34) combines the individual physicochemical molecular properties with the system thermodynamics. We can then compare the magnitude of these temperature induced fluctuations in the reaction rate constants, for each reaction, with the chiral bias induced by the PVED in that same reaction. This chiral selectivity criterion Eq. (62) compares the PVED bias (electroweak quantum chemistry) to the reaction transition state enthalpy (physical chemistry) and the medium's specific heat at constant volume (thermodynamics). All these factors affect the rate constant.

The simulations indicate the ability of the PVED bias to act as a good selector of the final stable chiral state depends on its magnitude and on the relative magnitude of the thermal fluctuations. This can be explained on the basis of the structure

of the imperfect bifurcation (see Appendix D). Indeed, an increase in the value of the PVED bias g translates the unstable scalemic branch down to more negative values of $\alpha < 0$ while the bifurcation point (where the unstable and stable scalemic branches meet) moves towards the right, to larger values of λ_c. This leads to a greater vertical distance between the racemic configuration at $\alpha = 0$ and the unstable scalemic branch. Hence it is more resilient to temperature fluctuations. On the other hand, smaller values of g have the opposite effect, moving the unstable scalemic branch upwards ever closer to the racemic configuration at $\alpha = 0$ and shifting the critical point λ_c to the left. Thus the system is now more sensitive to ever smaller temperature fluctuations about the racemic configuration. The simulations indicate that for PVED biases g greater than 10^{-19}, the amplification mechanism is resilient to thermal noise amplitudes ξ as much as an order of magnitude larger than g.

Temperature fluctuations directly affect the reaction rate constants, but not the numbers of molecules participating in the reactions, nor the system volume. The stochastic terms due to temperature fluctuations [Eqs. (9) and (34)] appearing in Eqs. (30)–(33) depend on the heat capacity at constant volume C_V, an extensive quantity, depending on system size, and system mass. So, we expect the *relative* temperature fluctuations decrease as system size increases, since the heat *capacity* increases with system size [Eq. (7)]. This is also true to a certain degree when the material, of which the reaction system is composed, has a large heat capacity. This latter point should be taken into account in proposals for possible experiments for the detection of the PVED as a selector of the chiral sign in SMSB scenarios. See Appendix B for details on the types of nonequilibrium fluctuations in open systems.

This in principle, allows us to study bounds on the absolute values of the transition state energies and enthalpies, mean temperatures, and the system's constant volume heat capacities, such that the maximum characteristic rate constant fluctuation, considering *all* the reactions i, is smaller than the constant PVED bias [Eq. (62)]. We then argue that the PVED bias should be detectable *macroscopically* in the overall reaction system, provided other sources of random fluctuations (e.g., in the particle numbers and in the volume) are quenched, or controlled and attenuated.

Interestingly, and apart from the still open question of whether the PVED itself has played any decisive role in determining the handedness of Earth's biochemistry, our paper points to a proposal for the design of a PVED detector, or more generally, a chiral bias detector. This is a special device operating under a specific regime of parameters, with a long duration constant flux in an open system. Yet, such an instrument is theoretically possible, and could be realized experimentally likely by exploiting small scale fluidic reactors, where there are no volume fluctuations and for which temperature and particle number fluctuations could be controlled and monitored. We envisage operation in the thermodynamic limit, where sufficiently large numbers validates the use of concentrations, and so suppresses reaction noise.

Our fluctuation analysis and simulation results differ markedly from those of earlier papers on this subject. First of all, we consider the competition between PVED selectivity and temperature fluctuations, with respect to an initial

nonequilibrium racemic composition. To ensure the initial racemic composition, a possibility is to start off without any flux (closed, batch reactor) and then initiate the flux rapidly, with a fast start. The results indicate a *nonlinear* relationship between the chiral bias and the temperature fluctuations. There is no direct way to relate fluctuations in chiral composition to temperature fluctuations. That is, even if we assume the local equilibrium hypothesis [27] and appeal to the Gibbs-Duhem relation, the latter only relates fluctuations in temperature to fluctuations in system pressure and to the overall net system composition, but not to *chiral* fluctuations themselves (see Appendix C). Thus, we need to translate δT into chiral fluctuations, and this requires direct simulation of the differential rate equations, which are stochastic by virtue of the fluctuating reaction rate constants.

In closing, we comment on the influence that various features may have on the robustness of our selectivity criterion Eqs. (62) and (63), and how their variability may affect some of the conclusions drawn in this paper, which uses a specific reaction model with certain kinetic parameters.

A. The values of the reaction rate constants

In the case of zero chiral bias, the reaction rate constants employed here place the Frank model on the unstable racemic branch. In the presence of PVED bias, the system is no longer located on any branch, but is instead initially within the basin of attraction of the stable scalemic branch selected by the bias (see Fig. 7 in Appendix D). The determinant factor for making the racemic branch unstable (zero bias case) is that the inverse rate of enantioselective autocatalysis over the forward rate of heterodimerization is less than unity, that is, $k_{-a}/k_1 < 1$. Note the latter rate is independent of the PVED bias, as it does not depend on g, whereas the former does (see Fig. 2). From Fig. 7 in Appendix D we see that PVED selectivity is relatively more favored the greater the distance between the initial racemic configuration and the unstable scalemic branch, so model parameters should be chosen accordingly, and such that the inequality Eq. (62) is obeyed. Since this distance goes to zero asymptotically as the system is driven further away from equilibrium (say, by increasing the flow rate), we expect PVED selectivity to also decrease in this limit. We have in fact observed this trend reflected clearly in the simulations reported in Sec. VI, where taking ever smaller PVED bias g shifts the initially racemic system closer to the unstable scalemic branch, making the system increasingly sensitive to ever smaller fluctuations (diminished selectivity).

B. The noise amplitude and frequency

The temperature fluctuations are modeled by white noise, characterized by an amplitude and a frequency [Eq. (8)]. The rms amplitude is determined by the constant volume heat capacity [Eq. (7)], and so depends on the composition of the solvent or medium as well as the system size. So, for a given medium, larger volumes imply smaller amplitude temperature fluctuations. The noise frequency ω should be chosen large enough such that $\omega \Delta t \gtrsim 1$, where Δt is the smallest time step used in the numerical solution of the differential rate equations. This is done to ensure randomness between

successive time steps. Smaller frequencies can lead to correlations between consecutive time steps, which could either have a constructive (reinforcing) or destructive (opposing) role with respect to the detection of the PVED bias.

C. Compositional vs temperature fluctuations

Fluctuations in the temperature δT are to be distinguished from compositional fluctuations, or fluctuations in the numbers δn_α of each species [see also Eq. (B3)]. The latter are characterized by the CLE, which is itself an approximation to the more fundamental chemical master equation [26]. Fluctuations in particle number are also known as reaction noise, and are a consequence of the fact that reactions involve individual molecules. This type of internal noise is suppressed in the thermodynamic limit, where both species number and system volume tend to infinity, while holding the ratio (number/volume), i.e., the concentration, constant. It is also suppressed in well-mixed homogeneous systems. Recently, a more involved but closed and kinetically controlled model for the Soai reaction was considered. Those authors estimated the minimum *binding energy* difference in product-initiator complexes required to break chiral symmetry in the presence of reaction noise (δn_α) [28].

D. System complexity

The Frank model involves five reversible reactions [Eqs. (15)–(17)], but only five independent rate constants (instead of ten) and a flow rate [Eqs. (18)–(22)]. The temperature fluctuations affect each individual rate constant, whereas the PVED bias only affects processes involving the enantiomers, such as direct production and enantioselective autocatalysis, but neither the forward nor reverse heterodimerization nor the flow rate (see Fig. 2). A more involved model with more reactions will have correspondingly more fluctuating rate constants. But of these, only a smaller subset will be independent, as dictated by chiral symmetry and thermodynamic constraints. Among these rate constants, the PVED bias only affects those processes involving single enantiomers. The selectivity criterion is applied to this set. Whether the bias g can overcome the noise depends on where the system is located with respect to the imperfect bifurcation. This initial position is model dependent; its location can in principle be determined in terms of the coefficients of the cubic bifurcation equation in Eq. (D1) in Appendix D (see also [8]).

E. Molecular modes

The parity-violating energy shift is itself a complicated function of the molecular geometry, and hence geometric distortions due to, for example, molecular vibration and rotation modes can lead to an implicit time dependence in the energy shift [29–31], and so in g. In the present paper, we assume these conformational fluctuations, about the molecular potential energy minimum, are negligible with respect to the temperature induced fluctuations in the reaction rate constants, and so regard the current quantum chemical computation estimates for E_{PV} in molecules to represent the mean values taken over large ensembles of molecules. This should

be a reasonable approximation for small system volumes, but large enough for the use of concentrations to be valid, i.e., in the thermodynamic limit.

F. Current estimates for g

Rough estimates for ξ are difficult to provide since these depend on the specific chemical reactions involved as well as on the system's heat capacity at constant volume. However, we can summarize briefly the history of the calculations for g. The possible connection of the PVED with handedness in biological molecules was first suggested in 1966 [4]. The theoretical framework for calculation PVED appeared in 1979 [32]. This framework was then used to carry out a "first generation" of PVED calculations using uncoupled-perturbed Hartree-Fock on a selection of biomolecules, yielding a g of order 10^{-17} [33,34]. The introduction of perturbative coupling in second generation calculations increased typical PVED values by one order of magnitude to $g = 10^{-16}$ [29–31,35]. Larger values of g may be obtained with molecules containing heavy atoms, and these calculations require using relativistic methods. In the case of the chiral molecule dihydrogen dipolonide H_2Po_2, $g = 10^{-9}$ is one of the highest reported calculated values for any molecule [36] [after conversion of E_{PV}(a.u.) to eV and with respect to room temperature]. Polonium ($Z = 84$) was chosen to demonstrate the higher than Z^5 scaling in the parity-violating energy difference in chiral molecules [36]. Finally, the asymmetric radiolysis of racemic mixtures of chiral molecules by spin-polarized electrons from beta decay, proposed in [4], was given a theoretical framework in [37]. The estimates from beta decay put $g \approx 10^{-12}$, and are still tentative; for a review see [35].

ACKNOWLEDGMENTS

APPENDIX A: RATE CONSTANT FLUCTUATIONS

Expanding $k(T)$ [Eq. (1)] for small relative temperature fluctuations $|\frac{\delta T}{T}| \ll 1$ leads to

$$
\begin{aligned}
k(T \pm \delta T) &= \frac{k_B(T \pm \delta T)}{h} e^{-\frac{(\Delta H^\ddagger - (T \pm \delta T)\Delta S^\ddagger)}{R(T \pm \delta T)}} \\
&= \frac{k_B(T \pm \delta T)}{h} e^{\frac{(-\Delta G^\ddagger \pm \delta T \Delta S^\ddagger)}{RT}} \left(1 \pm \frac{\delta T}{T}\right)^{-1} \\
&= \frac{k_B(T \pm \delta T)}{h} e^{\frac{(-\Delta G^\ddagger \pm \delta T \Delta S^\ddagger)}{RT}} \left(1 \mp \frac{\delta T}{T} + o\left(\left(\frac{\delta T}{T}\right)^2\right)\right) \\
&= \frac{k_B(T \pm \delta T)}{h} e^{-\frac{\Delta G^\ddagger}{RT} \pm \frac{\delta T}{T} \frac{\Delta G^\ddagger}{RT} \pm \frac{\delta T}{T} \frac{T\Delta S^\ddagger}{RT} + O((\frac{\delta T}{T})^2))} \\
&= \frac{k_B(T \pm \delta T)}{h} e^{-\frac{\Delta G^\ddagger}{RT}} e^{\pm \frac{\delta T}{T} \frac{\Delta H^\ddagger}{RT}} e^{o\left(\left(\frac{\delta T}{T}\right)^2\right)}
\end{aligned}
$$

$$
= \frac{k_B T \left(1 \pm \frac{\delta T}{T}\right)}{h} e^{-\frac{\Delta G^{\ddagger}}{RT}} \left(1 \pm \frac{\Delta H^{\ddagger}}{RT} \frac{\delta T}{T}\right.
$$

$$
+ O\left(\left(\frac{\delta T}{T}\right)^2\right)\Bigg)\Bigg)
$$

$$
= k(T) \left(1 \pm \left[1 + \frac{\Delta H^{\ddagger}}{RT}\right]\frac{\delta T}{T} + O\left(\frac{\delta T}{T}\right)^2\right). \tag{A1}
$$

The coefficient of unity in the brackets $[1 + ...]$ comes from expanding out the prefactor, but generally the ratio $\frac{\Delta H^{\ddagger}}{RT} \gg 1$ will be much greater (see examples in Table I, middle column, involving the transition energies).

APPENDIX B: TEMPERATURE FLUCTUATIONS IN OPEN SYSTEMS

The Einstein formula for the probability distribution of fluctuations in equilibrium

$$
P(\Delta S) = Z^{-1} e^{\Delta S / k_B}, \tag{B1}
$$

where ΔS is the entropy change associated with the fluctuation from equilibrium and Z is a normalization constant, was established for open nonequilibrium systems by Nicolis and Babloyantz (see [9,27]), and is valid in the range of the local equilibrium assumption. Einstein's formula shows that from thermodynamic entropy we can obtain the probability of fluctuations [10]. The entropy change with respect to a stationary state (NESS) is calculated to be

$$
\Delta_i S = -\frac{C_V (\delta T)^2}{2T^2} - \frac{1}{T\kappa_T} \frac{(\delta V)^2}{2V}
$$

$$
- \sum_{i,j} \left(\frac{\partial}{\partial N_j} \frac{\mu_i}{T}\right) \frac{\delta N_i \, \delta N_j}{2} < 0, \tag{B2}
$$

for fluctuations in the temperature δT and the volume δV and for the molar quantities δN_k. Here, we are interested in the temperature fluctuations in open systems.

Then the probability of a fluctuation in T, V, and N_k is given by (see Chap 14 in [10])

$$
P(\delta T, \delta V, \delta N_i) = Z^{-1} \exp(\Delta_i S / k_B) \tag{B3}
$$

$$
= Z^{-1} \exp\left[-\frac{C_V (\delta T)^2}{k_B \, 2T^2} - \frac{1}{T\kappa_T \, k_B} \frac{(\delta V)^2}{2V}\right.
$$

$$
- \sum_{i,j} \left(\frac{\partial}{\partial N_j} \frac{\mu_i}{T}\right) \frac{\delta N_i \, \delta N_j}{2k_B}\Bigg]. \tag{B4}
$$

The normalization factor is calculated from

$$
Z = \iiint P(x, y, z) \, dx \, dy \, dz. \tag{B5}
$$

Note, for a single variable X, the normal distribution with mean $\xi = \langle X \rangle$ and standard deviation σ is [38]

$$
\phi(X) = \frac{1}{\sqrt{2\pi}\sigma} e^{-\frac{1}{2}\left(\frac{X-\xi}{\sigma}\right)^2}
$$

$$
= \frac{1}{\sqrt{2\pi}\sigma} e^{-\frac{U^2}{2}}, \quad U = \left(\frac{X-\xi}{\sigma}\right). \tag{B6}
$$

Computing $P(\delta T)$ from above Eqs. (B4) and (B5) we find

$$
P(\delta T) = \frac{1}{\sqrt{2\pi}\sqrt{\frac{k_B}{C_V}}T} e^{-\frac{1}{2}\left(\frac{C_V (\delta T)^2}{k_B T^2}\right)}. \tag{B7}
$$

Using these expressions, we calculate the mean square temperature fluctuation:

$$
\langle (\delta T)^2 \rangle = \frac{k_B T^2}{C_V} = \sigma^2. \tag{B8}
$$

APPENDIX C: GIBBS-DUHEM RELATION

An important result from equilibrium thermodynamics is the Gibbs-Duhem relation which shows that *changes* in the intensive variables T, p, and μ_k cannot be all independent:

$$
S \, dT - V \, dp + \sum_k N_k \, d\mu_k = 0, \tag{C1}
$$

where S is the entropy, V the volume, N_k the molar quantity of kth species, and μ_k the chemical potential [10].

By using the *relative chemical potential* [39] (the concentration is $C_k = N_k / V$),

$$
\mu_k^{\text{rel}} = RT \ln\left(\frac{C_k}{C_k^{\text{eq}}}\right) = RT \ln\left(\frac{N_k}{N_k^{\text{eq}}}\right), \tag{C2}
$$

we can calculate the total change in μ_k to be

$$
d\mu_k^{\text{rel}} = \sum_j \left(\frac{\partial \mu_k^{\text{rel}}}{\partial N_j}\right) dN_j + \left(\frac{\partial \mu_k^{\text{rel}}}{\partial T}\right) dT \tag{C3}
$$

$$
= \sum_j \left(RT \frac{\delta_{jk}}{N_k}\right) dN_j + \left(\frac{\mu_k^{\text{rel}}}{T}\right) dT \tag{C4}
$$

$$
= RT \left(\frac{dN_k}{N_k}\right) + \left(\frac{\mu_k^{\text{rel}}}{T}\right) dT. \tag{C5}
$$

Substituting Eq. (C5) into Eq. (C1) yields

$$
\left[S + \sum_k \left(\frac{N_k \mu_k^{\text{rel}}}{T}\right)\right] dT - V \, dp + RT \sum_k dN_k = 0. \tag{C6}
$$

This relates fluctuations in the temperature, the pressure, and the molar amounts of all species involved. If we consider the NESS, where total chemical mass is constant, the fluctuations in the molar amounts [Eq. (C9)] are constrained as follows:

$$
[A]_{\text{in}} = [A] + [L] + [D] + 2[P] \tag{C7}
$$

$$
\Rightarrow N_{A\text{in}} = N_A + N_L + N_D + 2N_P \tag{C8}
$$

$$
\Rightarrow 0 = dN_A + dN_L + dN_D + 2 \, dN_P \tag{C9}
$$

for fixed input of A (clamped), which implies (and now assuming $dp = 0$)

$$
\left(S + \sum_k \left(\frac{N_k \mu_k^{\text{rel}}}{T}\right)\right) dT = RT \, dN_P. \tag{C10}
$$

So the Gibbs-Duhem relation, which is an equilibrium result, provides no information relating dT and *chiral* fluctuations: the dN_p are achiral fluctuations in the molar amount of the heterodimer. In order to relate dT to chiral fluctuations out of equilibrium, we must employ the kinetic rate equations, which is what we have done in the main paper.
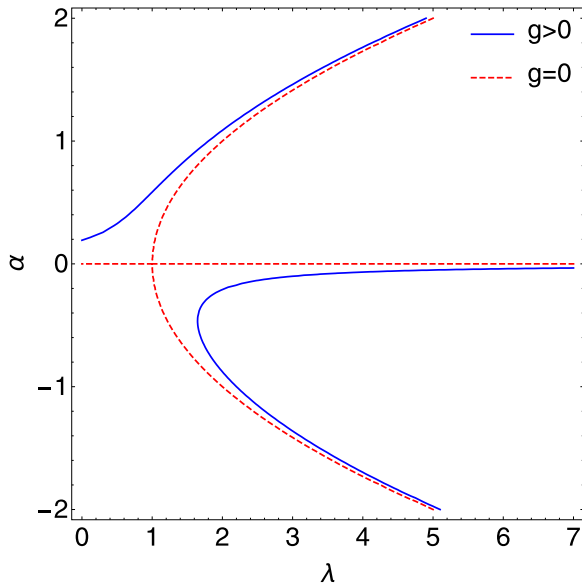
FIG. 7. Solution $\alpha(\lambda)$ of the bifurcation equation (D1). Red dashed curves: Perfect bifurcation in the absence of any chiral influence $g = 0$. Blue solid curves: The imperfect bifurcation diagram due to the chiral symmetry breaking interaction $g > 0$. Note that the racemic composition, or racemate, (represented by the abscissa $\alpha = 0$) is *not* a stationary solution of Eq. (D1) for $g > 0$, and hence does not form part of the imperfect bifurcation diagram. Instead, the racemate $\alpha = 0$ lies inside the basin of attraction of the upper stable scalemic branch (blue).

APPENDIX D: IMPERFECT BIFURCATION DUE TO CHIRAL BIAS

We review and compare the stability structure of the unbiased perfect bifurcation, with that of the biased *imperfect* bifurcation. From [10], the bifurcation of chiral symmetry breaking states is described by the following bifurcation equation:

$$-A\alpha^3 + B(\lambda - \lambda_c)\alpha + Cg = 0, \qquad (D1)$$

where $\alpha = ([L] - [D])/2$ is the chiral amplitude; $A > 0$, $B > 0$, and C are model dependent coefficients, functions of the concentrations, and reaction rates; and λ is a parameter representing the nonequilibrium constraint on the system (e.g., external clamped concentrations, flow rates, etc.). The parameter g is a small systematic bias. First suppose there is no such bias, so $g = 0$; then the solution of the resultant cubic equation Eq. (D1) includes the racemic branch $\alpha = 0$ and two mirror image stable scalemic branches, $\alpha_+ > 0$ and $\alpha_- = -\alpha_+ < 0$, that bifurcate off the racemic at the critical value $\lambda = \lambda_c$ (see dashed red lines in Fig. 7), in the plot $\lambda_c = 1$. For $\lambda < \lambda_c$ the only stationary solution is the stable racemic branch, whereas for $\lambda > \lambda_c$ the racemic branch becomes unstable, and both upper α_+ and lower α_- scalemic branches are stable. Which of the two stable scalemic branches the system evolves to is not deterministic, and cannot be predicted *a priori*, but depends on the random fluctuations about the unstable racemic branch. The outcome is stochastic, with an equal probability $p = \frac{1}{2}$ for the system to end up on either one of the stable scalemic branches.

In the presence of a small chiral bias $g \neq 0$, the stationary solutions of Eq. (D1) change qualitatively with respect to the unbiased case, depicted as shown in Fig. 7, and for $g > 0$. First, we note that the bifurcation, or critical point, gets shifted to the right: $\lambda_c(g) > \lambda_c(0) = 1$. This means the bias makes the upper scalemic branch relatively more stable, in that now we must drive the system *further* from equilibrium in order to have a possibility of a bifurcation. Second, in marked contrast to the unbiased case (dashed red lines), it is easy to check that the racemic composition $\alpha = 0$ is *not* a solution of Eq. (D1), for any value of λ, nor does the racemate belong to the thermodynamic branch. Instead, the upper stable scalemic $\alpha_+ > 0$ (upper blue curve) is the thermodynamic branch in the presence of bias. The racemate is not a *stationary* configuration. Rather, for $\lambda > \lambda_c(g)$ the system possesses three stationary scalemic branches (the upper and lower ones are stable, whereas the intermediate one is unstable). The (upper) scalemic branch favored by the bias exists for all λ, and tends towards the horizontal axis as the system approaches equilibrium, as $0 \leqslant \lambda < \lambda_c(g)$.

Moreover, as seen in Fig. 7, the racemic composition (the horizontal axis $\alpha = 0$) lies inside the basin of attraction of the upper stable scalemic branch. Hence, if the system is initially in a racemic configuration, and in the absence of fluctuations, it will evolve deterministically to this preferred stable scalemic branch. The bias selects this chiral branch for all values of λ, both below and above the critical value. In the presence of fluctuations, and for $\lambda < \lambda_c(g)$, the system will evolve to the (upper) stable scalemic branch selected by the bias, because this branch is the unique stable *attractor* in this domain. However, for $\lambda > \lambda_c(g)$ an initially racemic composition will only be able to evolve to the preferred scalemic branch if the bias g is able to overcome the temperature fluctuations around $\alpha = 0$. Temperature fluctuations lead to fluctuations in the reaction rate constants (see the main text), and the latter can lead, through nonlinearities, to chiral fluctuations in the compositions. For the (PVED) bias to be a good selector, fluctuations must not take the system into the basin of attraction of the *lower* stable scalemic branch. This other basin of attraction is separated from that of the upper stable scalemic branch by an intermediate *unstable* scalemic branch (see Fig. 7). When chiral bias fails to be a good selector, the system becomes stochastic; however, even for rate constant fluctuations on the same order of magnitude as the chiral bias $\xi \approx g$, the statistical distribution of the final stable scalemic outcomes can still reflect an appreciable amount of persistent and significant bias, and such that the two stable chiral outcomes are *not* equally likely. The outcomes follow a binomial distribution $P(n, p; k)$ where $0 \leqslant p \leqslant 1$ is the probability of one chiral outcome, and $q = 1 - p$ is the probability of the alternative chiral outcome but $p \neq q \neq 1/2$.

APPENDIX E: SYMMETRY BREAKING DUE TO TEMPERATURE FLUCTUATIONS

Further details of the evolution of the two enantiomers under the influence of temperature fluctuations alone show that the spontaneous mirror symmetry breaking can happen at different times, a purely stochastic phenomenon. To see this, it suffices to consider a simpler version of the open flow Frank
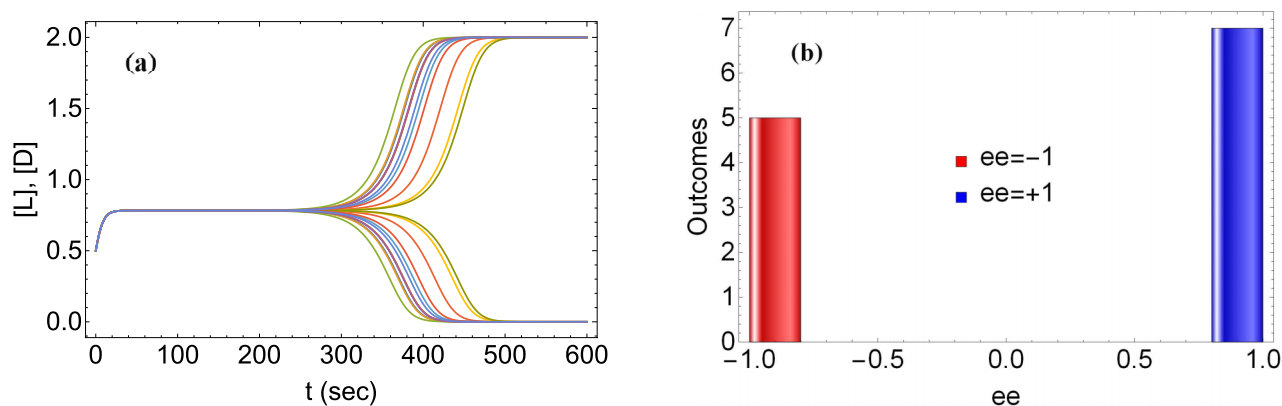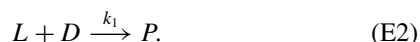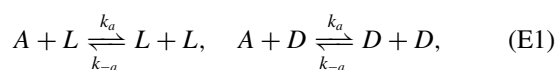
FIG. 8. Dynamic outcome of spontaneous mirror symmetry breaking triggered by pure temperature fluctuations in the rate constants, for the simplified open flow Frank model [Eqs. (E1) and (E2)]. (a) The evolution of both enantiomer concentrations $[L]$ and $[D]$ starting from an initial (unstable) racemic configuration for 12 independent runs. (b) The enantiomeric excess ee $= ([L] - [D]/[L] + [D])$ calculated at time $t = 600$ s. In these simulations, D is the majority enantiomer for five runs (ee $= -1$) and L is the majority for seven runs (ee $= +1$). $k_a(A) = 0.18$, $k_{-a} = 0.09$, $k_1 = 0.14$, initial $[L]_0 = [D]_0 = 0.5$, and noise amplitude $\xi = 10^{-6}$.

model considered in the main text. Essentially, we retain the reversible enantioselective autocatalysis and the forward rate of inhibition only. The system is open, as the input value of $[A]$ is clamped and we remove the inhibition product P. The steps are

$$A + L \underset{k_{-a}}{\overset{k_a}{\rightleftharpoons}} L + L, \quad A + D \underset{k_{-a}}{\overset{k_a}{\rightleftharpoons}} D + D, \qquad \text{(E1)}$$

$$L + D \xrightarrow{k_1} P. \qquad \text{(E2)}$$

For each individual run, the prevailing enantiomer can either be L or D. Already for a modest number of runs, there is a "pile-up" of majority and minority enantiomers for times subsequent to the symmetry breaking bifurcation [Fig. 8(a)]. The best way to tell which enantiomer prevails is to calculate the enantiomeric excess at an asymptotic time slice; these are plotted in Fig. 8(b), which exhibits the characteristic bimodal distribution.

[1] A. Guijarro and M. Yus, *The Origin of Chirality in the Molecules of Life* (Royal Society of Chemistry, Cambridge, England, 2009).

[2] F. Crick, *Life Itself: Its Origin and Nature* (Simon and Schuster, New York, 1981).

[3] P. D. B. Collins, A. D. Martin, and E. J. Squires, *Particle Physics and Cosmology* (Wiley, New York, 1989).

[4] Y. Yamagata, An hypothesis for the asymmetric appearance of biomolecules on earth, J. Theor. Biol. **11**, 495 (1966).

[5] T. L. V. Ulbricht and F. Vester, Attempts to induce optical activity with polarized β-radiation, Tetrahedron **18**, 629 (1962).

[6] M. Quack, How important is parity violation for molecular and biomolecular chirality?, Angew. Chem. Int. Ed. **41**, 4618 (2002).

[7] D. K. Kondepudi and G. W. Nelson, Chiral Symmetry Breaking in Nonequilibrium Systems, Phys. Rev. Lett. **50**, 1023 (1983).

[8] D. K. Kondepudi and G. W. Nelson, Chiral-symmetry-breaking states and their sensitivity in non-equilibrium chemical systems, Physica A **125**, 465 (1984).

[9] G. Nicolis and A. Babloyantz, Fluctuations in Open Systems, J. Chem. Phys. **51**, 2632 (1969).

[10] D. Kondepudi and I. Prigogine, *Modern Thermodynamics*, 2nd ed. (Wiley, New York, 2015).

[11] T. Shibata, H. Morioka, T. Hayase, K. Choji, and K. Soai, Highly enantioselective catalytic asymmetric automultiplication of chiral pyrimidyl alcohol, J. Am. Chem. Soc. **118**, 471 (1996).

[12] M. E. Noble-Terán, J. M. Cruz, J. C. Micheau, and T. Buhse, A Quantification of the Soai Reaction, ChemCatChem **10**, 642 (2018).

[13] O. Trapp, S. Lamour, F. Maier, A. F. Siegle, K. Zawatzky, and B. F. Straub, In situ mass spectrometric and kinetic investigations of soai's asymmetric autocatalysis, Chem. Eur. J. **26**, 15871 (2020).

[14] S. V. Athavale, A. Simon, K. N. Houk, and S. E. Denmark, Demystifying the asymmetry-amplifying, autocatalytic behaviour of the Soai reaction through structural, mechanistic and computational studies, Nat. Chem. **12**, 412 (2020).

[15] T. Buhse, J.-M. Cruz, M. E. Noble-Terán, D. Hochberg, J. M. Ribó, J. Crusats, and J.-C. Micheau, Spontaneous deracemizations, Chem. Rev. **121**, 2147 (2021).

[16] *Asymmetric Autocatalysis: The Soai Reaction*, edited by K. Soai, T. Kawasaki, and A. Matsumoto (Royal Society of Chemistry, Cambridge, England, 2022).

[17] R. Chang, *Physical Chemistry* (University Science, Sausalito, CA, 2000), Chap. 12.

[18] L. D. Landau and E. M. Lifshitz, *Statistical Physics*, 3rd ed. (Pergamon, New York, 1980), Vol. 1, Eq. (112.6).

[19] D. Todorović, I. Gutman, and M. Radulović, A stochastic chiral amplification model, Chem. Phys. Lett. **372**, 464 (2003).

[20] F. C. Frank, On spontaneous asymmetric synthesis, Biochim. Biophys. Acta **11**, 459 (1953).

[21] M. Stich, J. M. Ribó, D. G. Blackmond, and D. Hochberg, Necessary conditions for the emergence of homochirality via autocatalytic self-replication, J. Chem. Phys. **145**, 074111 (2016).

[22] These constraints were overlooked in [7,8] and are violated by the reaction rate constants used there.

[23] From Eqs. (15) and (16) and Eq. (34), the amplitudes satisfy $\xi_{\pm dL} = \xi_{\pm dD}$ for the forward and reverse direct production of enantiomers and $\xi_{\pm aL} = \xi_{\pm aD}$ for the forward and reverse auto-catalytic steps. The noise functions for each reaction (random process) remain statistically independent.

[24] M. Quack, J. Stohner, and M. Willeke, High-resolution spectroscopic studies and theory of parity violation in chiral molecules, Annu. Rev. Phys. Chem. **59**, 741 (2008).

[25] D. G. Blackmond, Autocatalytic models for the origin of biological homochirality, Chem. Rev. **120**, 4831 (2020).

[26] D. Gillespie, Stochastic simulation of chemical kinetics, Annu. Rev. Phys. Chem. **58**, 35 (2007).

[27] P. Glansdorff and I. Prigogine, *Thermodynamic Theory of Structure, Stability and Fluctuations* (Wiley, New York, 1971).

[28] N. A. Hawbaker and D. G. Blackmond, Energy threshold for chiral symmetry breaking in molecular self-replication, Nat. Chem. **11**, 957 (2019).

[29] P. Lazzeretti and R. Zanasi, On the calculation of parity-violating energies in hydrogen peroxide and hydrogen disulphide molecules within the random-phase approximation, Chem. Phys. Lett. **279**, 349 (1997).

[30] A. Bakasov and M. Quack, Representation of parity violating potentials in molecular main chiral axes, Chem. Phys. Lett. **303**, 547 (1999).

[31] F. Faglioni and P. Lazzeretti, Understanding parity violation in molecular systems, Phys. Rev. E **65**, 011904 (2001).

[32] D.W. Rein, R. A. Hegstrom, and P. G. H. Sandars, Parity non-conserving energy difference between mirror-image molecules, Phys. Lett. A **71**, 499 (1979).

[33] S. F. Mason and G. E. Tranter, The parity-violating energy difference between enantiomeric molecules, Mol. Phys. **53**, 1091 (1984).

[34] A. J. MacDermott, Electroweak enantioselection and the origin of life, Origins Life Evol. Biosphere **25**, 191 (1995).

[35] A. J. MacDermott, Comprehensive chirality, in *Perspective and Concepts: Biomolecular Significance of Homochirality: The Origin of the Homochiral Signature of Life*, edited by E. M. Carreira and H. Yamamoto (Elsevier, Amsterdam, 2012), Vol. 8, pp. 11–38.

[36] J. K. Laerdahl and P. Schwerdtfeger, Fully relativistic ab initio calculations of the energies of chiral molecules including parity-violating weak interactions, Phys. Rev. A **60**, 4439 (1999).

[37] R. A. Hegstrom, β Decay and the origins of biological chirality: Theoretical results, Nature (London) **297**, 643 (1982).

[38] G. A. Korn and T. M. Korn, *Mathematical Handbook for Scientists and Engineers* (Dover, New York, 2000), Chap. 18.

[39] D. Hochberg and J. M. Ribó, Stoichiometric network analysis of entropy production in chemical reactions, Phys. Chem. Chem. Phys. **20**, 23726 (2018).